DMD Fast Forward. Published on August 11, 2010 as doi:10.1124/dmd.110.033712

DMD #33712

Effects Of a Commonly Occurring Genetic Polymorphism of Human CYP3A4 (Ile118Val) On the Metabolism of Anandamide

Matthew Pratt-Hyatt, Haoming Zhang, Natasha T. Snider, and Paul F. Hollenberg

Primary Lab of Origin: Department of Pharmacology. University of Michigan School of Medicine, Ann Arbor, Michigan (MPH, HZ, PFH)

Department of Molecular & Integrative Physiology, University of Michigan School of Medicine, Ann Arbor, MI (NTS)

Running Title Page

Running Title: Human CYP3A4 (Ile118Val) Metabolism of Anandamide

Corresponding Author: Paul F. Hollenberg, PhD, Department of Pharmacology, The University of Michigan, 1150 W. Medical Center Dr. 2301 MSRB III, Ann Arbor, MI 48109-5632. Email: phollen@umich.edu.

Number of text Pages 24

Number of Tables 1

Number of Figures 9

References 28

Number of Words in Abstract 250

Number of Words in Introduction 418

Number of Words in Discussion 903

Abbreviations: AEA, anandamide; CB, cannabinoid receptor; CPR, cytochrome P450 reductase; EA, ethanolamide; EET, epoxyeicosatrienoic acid; 5,6-,8,9-,11,12-, and 14,15-EET-EAs; 5,6-,8,9-,11,12-, and 14,15-epoxyeicosatrienoic acid ethanolamides; ESI-LC/MS, electrospray ionization-liquid chromatography/mas spectrometry; HETE, hydroxyeicosatetraenoic acid; P450, cytochrome P450; THC, Δ-9-tetrahydrocannabinol; WT, wild type

Abstract

The endocannabinoid system plays an important role in numerous physiological processes including mood, appetite, and pain-sensation. A critical compound in maintaining cannabinoid tone is the endocannabinoid anandamide (AEA). We have recently shown that AEA is metabolized by several different human cytochrome P450s (P450) to form a number of metabolites; one of which exhibits an increased biological activity. CYP3A4, one of the major P450s involved in the metabolism of AEA, produces four major metabolites. One of these metabolites, 5,6 epoxyeicosatrienoic acid ethanolamide (5,6-EET-EA), exhibits a much higher affinity than AEA for the cannabinoid 2 receptor (CB-2) and leads to a marked decrease in intracellular cAMP levels in cells expressing CB-2. There are multiple human alleles of CYP3A4 and the CYP3A4.4 allele has been shown to exhibit a significant decrease in activity. Recombinant CYP3A4*4 was expressed in E.coli, and was demonstrated to produce 60% less 6-OH-testosterone than the wild type 3A4 (WT) in a reconstituted system. The metabolism of AEA by the WT and the CYP3A4.4 variant were investigated. The mutant produced 60% less of the four EET-EA metabolites than the WT. The mutant also produced a new peak on LC-MS not seen with the WT that corresponded to 19-HETE-EA. In addition, the mutant produces four novel peaks at m/z 380, which correspond to the addition of 2 oxygen atoms, possibly to form a peroxide bond. These data indicate that individuals expressing the CYP3A4.4 allele may exhibit significant variations in the metabolism of AEA as well as any other compounds resembling AEA.

DMD Fast Forward. Published on August 11, 2010 as DOI: 10.1124/dmd.110.033712
This article has not been copyedited and formatted. The final version may differ from this version.

Introduction

The endocannabinoid system is a multi-faceted signaling system that is located in many tissues in the body. Numerous recent results have illuminated how this complex system assists in controlling a wide variety of psychological and physiological processes including mood, appetite, inflammation, and pain-sensation (Richardson et al., 1998; Di Marzo et al., 2004).

Two (possibly three) receptors (CB1, CB2) have been discovered that bind either Δ-9-tetrahydrocannabinol (THC) or endogenous cannabinoids. CB1 has been found in numerous areas in the body such as the central nervous system, the cardiovascular system, and the peripheral nervous system (Felder et al., 2006). CB2 receptors are located primarily in cells in the immune system (Ducobu, 2005; Ducobu and Sternon, 2005; Vickers and Kennett, 2005; Felder et al., 2006).

The cannabinoid receptors are targets for a family of lipid transmitters. The first of these signaling molecules to be discovered was arachidonoylethanolamide, or anandamide (AEA), which is a derivative of arachidonic acid (Rodriguez de Fonseca et al., 2005). It has been found in numerous locations including the brain, plasma, and peripheral tissues. A novel pathway for AEA metabolism by human cytochrome P450s (P450) has recently been discovered (Snider et al., 2007). The primary P450 enzyme responsible for the oxidation of AEA in the liver is CYP3A4. This enzyme produces the four-monoepoxide molecules 5,6-, 8,9-,

11,12-, and 14,15-epoxyeicosatrienoic acid ethanolamides (EET-EAs). P450s 2D6 and also 4F2 metabolize AEA to produce the same four metabolites along with a fifth metabolite, 20-hydroxyeicosatetraenoic acid (HETE) (Snider et al., 2008). It has been hypothesized that the epoxygenated and hydroxylated compounds may be more potent ligands for cellular receptors than the parent AEA, and, in the case of 5,6-EET-EA, it has been demonstrated to have a higher affinity for the CB2 receptor than its parent AEA (Snider et al., 2009).

As indicated previously, P450 CYP3A4 is responsible for the majority of P450-catalyzed oxygenations of AEA in the liver. This enzyme has been shown to possess many single nucleotide polymorphisms (SNPs) in its coding region. One of these polymorphisms is CYP3A4*4, which has a frequency of 3.3% in the Chinese population (Wang et al., 2005). A protein product of this allele has been shown to possess a decreased catalytic activity. This allele also been reported to be correlated with an increase risk of subarachnoid hemorrhage in Japan with a P value for this correlation of 0.0006 (Yamada et al., 2008). This study provides insights into the ability of CYP3A4.4 to catalyze the metabolism of AEA and elucidates its altered pattern of AEA metabolites.

DMD Fast Forward. Published on August 11, 2010 as DOI: 10.1124/dmd.110.033712
This article has not been copyedited and formatted. The final version may differ from this version.

Material and Methods

Reagents. Anandamide, the various anandamide metabolite standards, and epoxide hydrolase were purchased from Cayman Chemical (Ann Arbor, MI). Catalase, NADPH, L-α-dilauroyl-phosphatidylcholine, L-α-dioleyl-sn-glycero-3-phosphatidylcholine, and L-α-phosphatidylserine were purchased from Sigma-Aldrich (St. Louis, MO). All other chemicals were of the highest quality and available from commercial sources.

Over-expression and Purification of CYP3A4, NADPH-dependent Cytochrome P450 Reductase, and Cytochrome b_5. The plasmid for the over-expression of CYP3A4 was a generous gift from Dr. James Halpert (University of California at San Diego, CA) (Domanski et al., 1998). CYP3A4 was expressed as a truncated form where the hydrophobic membrane-spanning domain was removed (Δ3-21) and several positively charged residues were introduced into the N-terminus to increase the expression yield. CYP3A4, cytochrome b_5, and cytochrome P450 reductase were expressed and purified as described previously (Hanna et al., 1998).

Site-directed Mutagenesis. The mutation of CYP3A4 was accomplished using the QuikChange site-directed mutagenesis kit according to the manufacturer's protocol (Stratgene, CA). The forward mutagenic primer was 5'-TTATGAAAAGTGCCGTCTCTATAGCTGAGGATG-3' and the reverse primer was 5'-CATCCTCAGCTATAGAGACGGCACTTTTCATAA-3.' The site-specific mutation was confirmed by DNA sequencing at the University of Michigan Sequencing Core facility.

Testosterone Metabolism. CYP3A4 protein was reconstituted with reductase and cytochrome b_5 (1:2:1 ratio), a 10-mg mixture of L-α-dilauroylphosphocholine, L-a-dioleyl-sn-glycero-3-phosphocholine, and L-α-phosphatidylserine (1:1:1), for 1 hour on ice. For the wild type and mutant proteins, 50 pmol of protein was used. Incubations were performed in reaction mixtures (1.0 ml) containing 50 mM HEPES buffer, pH 7.4, and 50 U of catalase. Reactions were initiated by the addition of NADPH to give a final concentration of 1.2 mM. Control reactions were done in the absence of NADPH. Incubations were conducted for 10, 20, and 40 minutes in triplicate. Samples were terminated and extracted with ethyl acetate and dried under nitrogen. They were then resuspended in 150 ml of 65% methanol and 90 µl fractions were then injected into a Shimadzu HPLC (Shimadzu Scientific Instrument, Columbia, MD). The metabolites were resolved isocratically on a C18 reverse phase column (Varian, Walnut Creek, CA) equilibrated with 62% methanol and eluted using a flow rate of 1ml/min. Metabolites were detected at 254 nm and were quantitated using a standard curve constructed using known amounts of 6-β-OH- testosterone.

Anandamide Metabolism Assays. CYP3A4 was reconstituted with reductase and phospholipid as stated previously. Studies were performed using incubation mixtures (0.5 ml) containing 50 mM HEPES buffer, pH 7.4, and 50 U of catalase. Experimental reactions were initiated by the addition of NADPH to give a final concentration of 1.2 mM. Control reactions were done in the absence of NADPH. Samples were incubated at 37^{o}C. The reactions were terminated by the addition of 3 ml of nitrogen-purged ethyl acetate. Samples were vortexed for

1 minute and then centrifuged for 5 min at 1200 rpm to separate the organic layer. This layer was removed, dried under a constant stream of nitrogen, resuspended in160 μl of methanol, and 20 μl-fractions were subjected to electrospray ionization liquid chromatography/mass spectrometry (ESI-LC/MS) analysis as described below.

For determinations of the K_m and V_{max} values, the incubation conditions were optimized for time and protein concentration and performed within the linear range for metabolite formation. For these studies, 30 pmol of CYP3A4 protein in the reconstituted system was incubated with AEA at the concentrations indicated for 20 minutes. After extraction with nitrogen-purged ethyl acetate and drying, the extracts were resuspended in 160 μl of methanol and 20 μl aliquots were injected for analysis by ESI-LC/MS. The AEA peak was used as the internal standard because under reaction conditions the amount metabolized was always less than 5% of the total amount (Supplemental Figure). Standard curves for 5,6-, 8,9-, 11,12-, and 14,15-EET-EA were generated by injecting known amounts of the standards (Cayman Chemicals) into the ESI-LC/MS. For reactions containing recombinant epoxide hydrolase (EH), CYP3A4.4 (50 pmol) was incubated in the above reaction mixture with recombinant EH (25 pmol) for 2 hours at 37^{o}C.

ESI-LC/MS Analysis of AEA metabolism. Samples (20 μl of each) were injected onto a Hypersil ODS column (5 μm, 4.6x100 mm; Thermo Fisher Scientific, Waltham, MA) that had been equilibrated with 75% solvent B (0.1% acetic acid in methanol) and 25% solvent A (0.1% acetic acid in water). The

metabolites were resolved using the following gradient: 0 to 5 min, 75% B; 5 to 20 min, 75 to 100% B; 20 to 25 min, 100% B; 25 to 26 min, 100 to 75% B; and 26 to 30 min, 75% B. The flow rate was 0.3 ml/min. The column effluent as directed into the LCQ mass analyzer (Thermo Electron Corporation, Waltham, MA). The ESI conditions were as follows: sheath gas, 90 arbitrary units; auxiliary gas, 30arbitrary units; capillary temperature, 200 ^{o}C; and spray voltage, 4.5 KV. Data were acquired in positive ion mode using Xcalibur software package (Thermo Electron Corporation) with one full scan from 300 to 500 mass to charge ratio (m/z) followed by one data dependent scan of the most intense ion.

Data Analysis. Nonlinear regression analyses of the data were performed using Graphpad Prism version 5 for Mac (Graph Pad Software, La Jolla CA; www.graphpad.com).

Docking of Anandamide into CYP3A4. AEA was docked into the active site of CYP3A4 as a flexible ligand using Autodock software 4.0 (Morris et al., 1996). The coordinates of CYP3A4 were obtained from the protein data bank (ID code 1TQN). The water molecules were removed from the coordinates prior to docking. The coordinates for the AEA were constructed using ChemOffice suite 2008 (CambridgeSoft, MA) and the geometry of AEA was optimized with the semi-empirical QM method AM1. Due to the large number of rotatable bonds in AEA, the docked conformations were not well clustered. Therefore prediction of the metabolites of AEA is poor. The selected pose of AEA shown in Figure 3

represents one possible conformation of the bound AEA that leads to the formation of 11,12-EET-EA.

Metabolism of the AEA metabolites with m/z 380 by prostaglandin D synthase (PGDS) CYP3A4.4 protein (240 pmol) was reconstituted with reductase and cytochrome-b_5 as previously stated in a final volume of152 μl. To eight 0.5 ml reaction mixtures 20 μl each of the reconstitution mix was added to samples containing 50 mM HEPES, pH 7.4, 100 μM AEA, and 50 U of catalase. NADPH was added to each of the reactions to give a final concentration of 1.2 mM and the samples were incubated at 37^{o}C for 20 min. Reactions were terminated by the addition of 2 ml of nitrogen-purged ethyl acetate and the samples were extracted and dried as described previously. All 8 samples were resuspended in 15 μl of 50% methanol each and pooled. The pooled samples were then added to 100 mM Tris buffer, pH 8.0, containing 2 mM $MgCl_2$ and 2 mM GSH in a final volume of 0.5 ml. In the control samples, 10 μl of 100 mM Tris was added and in experimental samples, 10 μl of 0.5 μg/μl of prostaglandin D synthase in 100 mM Tris was added. Samples were incubated for 30 min at room temperature and then the reactions were terminated with ethyl acetate. Samples were then analyzed by LC/MS as previously indicated.

Spectral Properties. To analyze the spectral binding of AEA to P450 3A4 and the CYP3A4.4 mutant, the spectra were measured using previously published methods (Estabrook and Werringloer, 1978; Shebley and Hollenberg, 2007). P450 3A4 and the 3A4.4 polymorphic form were diluted in 50 mM KPi, pH 7.4, to

a final concentration of1μM in a final volume of 2 ml and equal volumes of each were placed in the reference and sample cuvettes. A difference spectrum between the two cuvettes was recorded from 350 to 700 nm on a UV-2501PC spectrophotometer (Shimadzu, Kyoto, Japan). Increasing concentrations of AEA (1 μM-100 μM) in methanol were added to the sample cuvette, while the reference cuvette received equal volumes of methanol and the difference spectra were determined after each addition and the spectral K_s values were calculated as described previously.

Measurements of Rates of Electron Transfer by Stopped-flow Spectrophotometry. The rates of reduction of the wild type and the mutant P450 were determined at 25^{o}C using a Hi-Tech SF61DX2 stopped-flow spectrophotometer (Hi-Tech, Wiltshire, UK) as previously described (Zhang et al., 2008). The CYP3A4 (3 μM) was reconstituted with 3 μM cytochrome P450 reductase (CPR) and 10 μg/mL of lipid in 50 mM HEPES buffer, pH 7.4, in a final volume of 2 ml on ice for 60 minutes. After reconstitution for 60 minutes, the protein samples were bubbled with CO gas for 6 minutes and then loaded into a syringe of the stopped-flow spectrophotometer. CO-saturated HEPES buffer, pH 7.4, containing 0.1 mM NADPH was loaded into a second syringe. The kinetic traces at 450 nm were recorded after rapid mixing of the contents of both syringes. Four shots with CYP 3A4 were performed and scanned for 120 s each. Four shots were performed using CYP3A4.4 and they were scanned for 1200 s each.

Results

Mutation of residue 118 from Leucine to Valine in human CYP3A4 causes a decrease in catalytic activity. To investigate the activity of the mutant compared to the wild type we analyzed its ability to metabolize testosterone to form 6-β-OH-testosterone.Using 50 pmole samples of wild type and mutant P450s we determined that the mutant possessed approximately 33% of the activity of the wild type (Figure 1).

As shown previously, CYP3A4 metabolizes AEA to form four monoepoxide molecules(Snider et al., 2007; Snider et al., 2008). These metabolites are the 5,6-, 8,9-, 11,12-, and 14,15-EET-EA and they are formed in a time and protein concentration dependent manner. Using expressed human CYP3A4*1 and CYP3A4*4 purified from E.coli, we performed kinetic analyses on the formation of these metabolites from AEA at concentrations ranging from 1to 125 μM. Using optimized conditions for the incubation time and protein concentration we determined that formation of the 5,6-, 8,9-, 11,12-, and 14,15-EET-EA all exhibited Michaelis-Menten kinetics (Figure 2) and the values calculated for K_m and V_{max} from these data are presented in Table 1. These data demonstrate that the CYP3A4*4 polymorphism causes approximately one and a half to three-fold decreases in the V_{max} values for the formation of the four primary metabolites of AEA. Except for the 8,9-EET-EA metabolite, where the K_m increased by a factor of 2, the K_m values for all of the other metabolites were relatively unchanged.

The CYP3A4.4 variant exhibits an increase in the formation of dioxygenated products as well as an additional monoxygenated metabolite of AEA. As reported previously, wild type CYP3A4 primarily forms four epoxide metabolites of AEA (Snider et al., 2007). Since the 118 residue is near the active site and might be predicted to alter the binding of AEA (Figure 3) we investigated the possibility that the amounts of the products or the ratios of metabolites formed during AEA metabolism might differ from the CYP3A4 wild type. The ratio of metabolites for the original epoxides was unchanged; however, AEA metabolism by the mutant protein resulted in the formation of one additional monoxygenated product with an m/z at 364, indicated as M5 in Figure 4B, and four previously unreported dioxygenated products with m/z values at 380, indicated as M1-M4 in Figure 4A. The monoxygenated product is most likely 19-HETE-EA based on its retention time on the C18 column (Nithipatikom et al., 2001). Wild type CYP3A4 does not produce this metabolite; however, it has previously been observed as a metabolite of AEA that is formed by human liver microsomes (Snider et al., 2007).

The four dioxygenated products (M1-M4) were formed in quantities comparable to the monoxygenated products (M6-M9) by the 3A4.4 mutant protein; however, the dioxygenated products were produced in relatively small quantities by the wild type when compared to the epoxygenated products. The peaks for the dioxygenated products produced by the mutant protein were more than 10 times greater than those formed by the wild type. We initially hypothesized that these dioxygenated products were formed by a subsequent

oxygenation of the monoxygenated products. In order to investigate whether these products might have been produced by a second oxygenation of the monoxygenated products (M6-M9) we incubated the monoxygenated products with CYP3A4.4 to determine if any of the dioxygenated products observed would be formed. After forty minute incubations we examined the samples by LC-MS and observed that the incubations with these substrates did not produce any of the dioxygenated products (M1-M4) (data not shown). These results led us to hypothesize that the dioxygenated products may be produced directly from AEA by the 3A4.4 mutant protein.

The novel products M1-M5 formed from AEA by CYP3A4.4 are not epoxides. The possibility that the novel monoxygenated product and that the dioxygenated products might be epoxides was then investigated. CYP3A4.4 was incubated with AEA in the presence of added epoxide hydrolase (EH) (Cayman) as described previously, (Snider et al., 2007). As illustrated in Figure 5, the M5 peak with m/z 364 did not decrease when incubated in the presence of EH; however, we did observe the expected decreases in peaks M6-M9 as demonstrated previously (Snider et al., 2007). In addition, we observed no decrease in the intensity of the M1-M4 peaks (results not shown), which indicates that these products are not epoxides.

The novel M1-M4 products formed from AEA by CYP3A4.4 are further metabolized by prostaglandin D synthase. Since M1-M4 were unaffected by EH, we hypothesized that these novel peaks might be the result of formation of a peroxide bond on AEA. To test this hypothesis these metabolites were incubated

with prostaglandin D synthase (PGDS), which catalyzes the cleavage of the peroxide bond present in prostaglandin H_2 (Watanabe et al., 1980). For these studies, the CYP3A4.4 M1-M4 metabolites of AEA were formed by incubation of the AEA with the 3A4.4, isolated and then incubated with PGDS for 30 min and then examined by LC/MS. The M1-M4 product peaks decreased after incubation with PGDS and a new peak (M14) with m/z 381 was observed (Figure 6). These results suggest that the peroxide bond was broken to form an alcohol as well as a ketone bond, as has been observed for the metabolism of the peroxide bond in prostaglandin H_2 by PGDS. These results indicate that these novel peaks (M1-M4) may possess peroxide bonds.

Mutation of Ile 118 to Val changes the environment of the heme. Analysis of the crystal structure of CYP3A4 suggested that the Ile188 to Val mutation might have an effect on the heme since the side chain of Ile118 is only 3.8 A away from the pyrrole D ring of the heme (figure 3). Therefore, we analyzed the UV-visible spectra of both the wild type and the Ile118Val mutant (Figure 7). The spectra of both were determined in the presence and absence of AEA. The spectrum of wild type CYP3A4 exhibits a mix of both high and low spin heme iron with the absorption maximum being at 424 nm. Spectral titration of the wild type enzyme with AEA gave a spectral K_s of 1.8μM for AEA (data not shown). The mutant exhibited a predominantly low spin spectrum with a maximum at 427 nm and there was no change in the UV-spectrum following the addition of AEA. Therefore, we were unable to determine a K_s for AEA binding to the mutant.

Mutation of residue 118 from Ile to Val in 3A4 causes a decrease in the rate of reduction. In order to investigate the basis for the lowered catalytic activity for the monoxygenation of testosterone and AEA by the mutant, we measured the rate of electron transfer from CPR to the ferric CYP3A4. These experiments were done in the presence and absence of 100 μM testosterone. The results are shown in Figure 8. The wild type 3A4A without testosterone (Figure 8A empty circles) demonstrates a biphasic kinetic trace. Fitting of the kinetic trace with two exponentials gives the apparent rate constants (k_{obs}) of 0.15 for the fast phase and 0.0026 s^{-1} for the slow phase. In contrast, the mutant protein (Figure 8B) shows monophasic kinetics with a k_{obs} of 0.0002 s^{-1}, which is approximately 750–fold slower than the fast phase of the wild type. This demonstrates a very significant decrease in the rate of the first electron transfer from CPR to the mutant. In addition, the wild type demonstrates an increase in rate of transfer in the presence of testosterone (Figure 8A filled circles), while the mutant protein is unaffected by the presence of testosterone (Figure 8B).

Discussion

The results presented here demonstrate that the Ile118Val mutation has a profound effect on the metabolism of AEA by CYP3A4. Not only does the mutation lower its activity for the metabolism of AEA, but it also causes changes in the ratios of the monoxygenated metabolites formed as well as leading to the formation of a new monoxygenated metabolite and four new dioxygenated metabolites. Besides changes in AEA metabolism, we also observed that the mutation results in a lowered rate of metabolism for testosterone, as well as lower rates of metabolism for other CYP3A4 substrates such as verapamil, tamoxifen, and ritonavir (data not shown).

UV spectral analysis of CYP3A4.1 and CYP3A4.4 indicate that this SNP in CYP3A4.4 also leads to a significant change in the interactions between the apoprotein and the heme. The spectral results showing that the variant has an increased low spin character suggest that the bond at the axial position between the heme and the apoprotein may have been strengthened significantly. The results from the stopped flow studies also indicate that the rate of the flow of electrons from the reductase to the P450 for the reduction by the ferric iron by the first electron has been hindered significantly. This hindrance is most likely due to the modulation of the redox potential of the heme by the Ile118Val mutation because of its proximity to the heme. This mutation could also result in greater access of water to the active site. These data support the possibility that

changes in the environment of the heme due to the mutation may in part be responsible for the significant decrease in catalytic activity.

Understanding this and other P450 polymorphisms may prove to be very helpful in understanding disease states in numerous tissues and their responses to drugs as well as in the development of novel therapeutics. Previous studies have demonstrated that AEA is metabolized to give the five primary metabolites identified here in several different tissues; most importantly in the liver and the brain. In the liver and brain, AEA is metabolized to form multiple products. It has been further demonstrated that CYP3A4 is involved in the formation of these products in both tissues. Studies have shown that the addition of antibodies to CYP3A4 to brain microsomes results in a significant decrease in the formation of AEA metabolites (Bornheim et al., 1995; Snider et al., 2007). The novel monooxygenated product produced by the Ile118Val mutant corresponds to the 19-HETE-EA product observed previously following AEA metabolism by murine BV-2 microglial cells (Snider et al., 2009).

The other four novel products produced by the Ile118Val mutant may potentially be very important biological metabolites. Our results demonstrate that these products result from the addition of two oxygens. Since these products are not further metabolized by epoxide hydrolase, they are not products formed by the epoxidation of two different double bonds. This lead us to hypothesize that these molecules might be due to the formation of a peroxide bond similar to that in prostaglandin H_2, which is formed from arachidonic acid by the enzyme cyclooxygenase. Prostaglandin H_2 is a precursor for many different molecules

that are important for numerous functions such as inflammation, renal function, blood clotting, and the maintenance of the gastrointestinal tract (Simmons et al., 2004). Thus, we have hypothesized that these four products (M1-M4) are the result of CYP3A4 forming peroxide bonds at each of the four double bonds of AEA. The partial disappearance of all four of these metabolites following incubation with prostaglandin D synthase supports the suggestion that these metabolites are peroxides (Figure 9).

AEA as well as some of its metabolites have been shown to bind to multiple types of receptors. Progress has been made to elucidate the compounds that bind to these receptors and the physiological results of binding. The two most studied cannabinoid receptors, CB1 and CB2, have different binding affinities for AEA and its metabolites. CB1, is found in the brain as well as in other tissues, (Palmer et al., 2000; Kozak and Marnett, 2002; Snider et al., 2009), and has been demonstrated to be involved in the cannabinoid signaling pathway that protects against stroke in mice (Parmentier-Batteur et al., 2002; Marsicano et al., 2003; Panikashvili et al., 2005). The second receptor, CB2, is involved in inflammation and agonists targeting CB2 are currently being developed as therapies to reduce inflammation and pain (Whiteside et al., 2005). It has recently been shown that the metabolism of AEA by CYP3A4 can form at least one product, 5,6-EET-EA, which has a significantly increased binding affinity for CB2. This binding has also been shown to be very selective for CB2 over CB1(Snider et al., 2009). Two other receptors that seem to play roles in AEA signaling are the vanilloid receptors and a non-CB1/non-CB-2 cannabinoid

receptor. These receptors are believed to play roles in mediating AEA dependent vasorelaxant effects (De Petrocellis et al., 2001; Herradon et al., 2007).

P450 3A4 produces a variety of different mono- and dioxygenated metabolites from AEA. These results demonstrate the formation of nine different oxygenated metabolites from AEA. Studies aimed at elucidating the structures of the five new metabolites of AEA reported here, their presence in various tissues, and their physiological roles are important for a comprehensive understanding the endocannabinoid signaling system. Future studies will investigate the possible biological activity of the new CYP3A4 metabolites and the consequences of the CYP3A4.4 mutation on the regulation of the cannabinoid signaling system.

Acknowledgments

We thank Drs. Mike Tarasev and David Ballou for help with stopped-flow experiments.

References

Bornheim LM, Kim KY, Chen B and Correia MA (1995) Microsomal cytochrome P450-mediated liver and brain anandamide metabolism. *Biochem Pharmacol* **50:**677-686.

De Petrocellis L, Bisogno T, Maccarrone M, Davis JB, Finazzi-Agro A and Di Marzo V (2001) The activity of anandamide at vanilloid VR1 receptors requires facilitated transport across the cell membrane and is limited by intracellular metabolism. *J Biol Chem* **276:**12856-12863.

Di Marzo V, Bifulco M and De Petrocellis L (2004) The endocannabinoid system and its therapeutic exploitation. *Nat Rev Drug Discov* **3:**771-784.

Domanski TL, Liu J, Harlow GR and Halpert JR (1998) Analysis of four residues within substrate recognition site 4 of human cytochrome P450 3A4: role in steroid hydroxylase activity and alpha-naphthoflavone stimulation. *Arch Biochem Biophys* **350:**223-232.

Ducobu J (2005) [The endocannabinoid system and the regulation of the metabolism]. *J Pharm Belg* **60:**84-88.

Ducobu J and Sternon J (2005) [Rimonabant (Acomplia), specific inhibitor of the endocannabinoid system]. *Rev Med Brux* **26:**165-168.

Estabrook RW and Werringloer J (1978) The measurement of difference spectra: application to the cytochromes of microsomes. *Methods Enzymol* **52:**212-220.

Felder CC, Dickason-Chesterfield AK and Moore SA (2006) Cannabinoids biology: the search for new therapeutic targets. *Mol Interv* **6:**149-161.

Hanna IH, Teiber JF, Kokones KL and Hollenberg PF (1998) Role of the alanine at position 363 of cytochrome P450 2B2 in influencing the NADPH- and hydroperoxide-supported activities. *Arch Biochem Biophys* **350:**324-332.

Herradon E, Martin MI and Lopez-Miranda V (2007) Characterization of the vasorelaxant mechanisms of the endocannabinoid anandamide in rat aorta. *Br J Pharmacol* **152:**699-708.

Kozak KR and Marnett LJ (2002) Oxidative metabolism of endocannabinoids. *Prostaglandins Leukot Essent Fatty Acids* **66:**211-220.

Marsicano G, Goodenough S, Monory K, Hermann H, Eder M, Cannich A, Azad SC, Cascio MG, Gutierrez SO, van der Stelt M, Lopez-Rodriguez ML, Casanova E, Schutz G, Zieglgansberger W, Di Marzo V, Behl C and Lutz B (2003) CB1 cannabinoid receptors and on-demand defense against excitotoxicity. *Science* **302:**84-88.

Morris GM, Goodsell DS, Huey R and Olson AJ (1996) Distributed automated docking of flexible ligands to proteins: parallel applications of AutoDock 2.4. *J Comput Aided Mol Des* **10:**293-304.

Nithipatikom K, Grall AJ, Holmes BB, Harder DR, Falck JR and Campbell WB (2001) Liquid chromatographic-electrospray ionization-mass spectrometric analysis of cytochrome P450 metabolites of arachidonic acid. *Anal Biochem* **298:**327-336.

Palmer SL, Khanolkar AD and Makriyannis A (2000) Natural and synthetic endocannabinoids and their structure-activity relationships. *Curr Pharm Des* **6:**1381-1397.

Panikashvili D, Mechoulam R, Beni SM, Alexandrovich A and Shohami E (2005) CB1 cannabinoid receptors are involved in neuroprotection via NF-kappa B inhibition. *J Cereb Blood Flow Metab* **25:**477-484.

Parmentier-Batteur S, Jin K, Mao XO, Xie L and Greenberg DA (2002) Increased severity of stroke in CB1 cannabinoid receptor knock-out mice. *J Neurosci* **22:**9771-9775.

Richardson JD, Kilo S and Hargreaves KM (1998) Cannabinoids reduce hyperalgesia and inflammation via interaction with peripheral CB1 receptors. *Pain* **75:**111-119.

Rodriguez de Fonseca F, Del Arco I, Bermudez-Silva FJ, Bilbao A, Cippitelli A and Navarro M (2005) The endocannabinoid system: physiology and pharmacology. *Alcohol Alcohol* **40:**2-14.

Shebley M and Hollenberg PF (2007) Mutation of a single residue (K262R) in P450 2B6 leads to loss of mechanism-based inactivation by phencyclidine. *Drug Metab Dispos* **35:**1365-1371.

Simmons DL, Botting RM and Hla T (2004) Cyclooxygenase isozymes: the biology of prostaglandin synthesis and inhibition. *Pharmacol Rev* **56:**387-437.

Snider NT, Kornilov AM, Kent UM and Hollenberg PF (2007) Anandamide metabolism by human liver and kidney microsomal cytochrome p450 enzymes to form hydroxyeicosatetraenoic and epoxyeicosatrienoic acid ethanolamides. *J Pharmacol Exp Ther* **321:**590-597.

Snider NT, Nast JA, Tesmer LA and Hollenberg PF (2009) A cytochrome P450-derived epoxygenated metabolite of anandamide is a potent cannabinoid receptor 2-selective agonist. *Mol Pharmacol* **75:**965-972.

Snider NT, Sikora MJ, Sridar C, Feuerstein TJ, Rae JM and Hollenberg PF (2008) The endocannabinoid anandamide is a substrate for the human polymorphic cytochrome P450 2D6. *J Pharmacol Exp Ther* **327:**538-545.

Vickers SP and Kennett GA (2005) Cannabinoids and the regulation of ingestive behaviour. *Curr Drug Targets* **6:**215-223.

Wang A, Yu BN, Luo CH, Tan ZR, Zhou G, Wang LS, Zhang W, Li Z, Liu J and Zhou HH (2005) Ile118Val genetic polymorphism of CYP3A4 and its effects on lipid-lowering efficacy of simvastatin in Chinese hyperlipidemic patients. *Eur J Clin Pharmacol* **60:**843-848.

Watanabe K, Shimizu T, Iguchi S, Wakatsuka H, Hayashi M and Hayaishi O (1980) An NADP-linked prostaglandin D dehydrogenase in swine brain. *J Biol Chem* **255:**1779-1782.

Whiteside GT, Gottshall SL, Boulet JM, Chaffer SM, Harrison JE, Pearson MS, Turchin PI, Mark L, Garrison AE and Valenzano KJ (2005) A role for cannabinoid receptors, but not endogenous opioids, in the antinociceptive activity of the CB2-selective agonist, GW405833. *Eur J Pharmacol* **528:**65-72.

Yamada Y, Metoki N, Yoshida H, Satoh K, Kato K, Hibino T, Yokoi K, Watanabe S, Ichihara S, Aoyagi Y, Yasunaga A, Park H, Tanaka M and Nozawa Y (2008) Genetic factors for ischemic and hemorrhagic stroke in Japanese individuals. *Stroke* **39:**2211-2218.

Zhang H, Hamdane D, Im SC and Waskell L (2008) Cytochrome b5 inhibits electron transfer from NADPH-cytochrome P450 reductase to ferric cytochrome P450 2B4. *J Biol Chem* **283:**5217-5225.

Footnotes

A. Funding: This work was supported in part by a Biology of Drug Abuse Postdoctoral training fellowship from the National Institute of Drug Abuse [DA007268-18] to MPH, NTS was supported by the Michigan Institute for Clinical and Health Research Postdoctoral Translational Scholars Program [Award UL1-RR024986] as well as a grant from the National Institutes of Health [CA016954] to PFH

B. Please send reprint requests to: Paul F. Hollenberg, PhD, Department of Pharmacology, The University of Michigan, 1150 W. Medical Center Dr. 2301 MSRB III, Ann Arbor, MI 48109-5632. Email: phollen@umich.edu.

Figure Legends

Figure 1. Formation of 6-β-OH-testosterone by CYP3A4 and the Ile228Val mutant. Reaction mixtures contained 50 pmol of the wild type 3A4 (●) or the Ile 118Val variant (■) P450 proteins in the reconstituted system and 100μM testosterone. Reactions were incubated and then analyzed after 0, 20, and 40 minutes as described in Materials and Methods. The amount of product formed was determined based on a standard curve generated using 6-β-OH-testosterone.

Figure 2. Kinetics for the formation of the metabolites of AEA by human recombinant CYP3A4.1 and CYP3A4.4. Reaction mixtures contained 30 pmol CYP3A4.1(A) or CYP3A4.4.4 (B) and the reconstituted system as described in Material and Methods. The AEA concentrations were 1-256μM(A) and 1-128 μM(B) and the reaction mixtures were incubated for 20 min at 37^{o}C. The metabolites of AEA that were quantified were 14,15-EET-EA(●),11,2-EET-EA(■),8,9-EET-EA(▲),5,6-EET-EA(▼). The amounts of products formed were determined based on standard curves generated for each metabolite, and the rate data (the average of six experiments) were fitted to a one-enzyme Michaelis-Menten model using Prism software.

Figure 3. Molecular modeling results showing AEA (purple) bound into the active site of CYP3A4. The coordinates for CYP3A4 were obtained from the Protein Data Bank and AEA was docked into CYP3A4 using Autodock. Residue118 is located in close proximity of the heme (red). Mutation of this

residue possibly changes the conformation of the active site, thus affecting CYP3A4 activity.

Figure 4. Metabolism of AEA by CYP3A4.1 and CYP3A.4. Reaction mixtures containing 30 pmol of CYP3A4.1 or CYP3A4.4 in the reconstituted system described in Material and Methods and containing 64 μM AEA were incubated for 20 min at 37^{o}C. Peaks were normalized to the AEA peak (not shown). Reactions done in the absence of NADPH contained only the AEA peak (not shown) (A) Polymorphic CYP3A4.4 produces significantly more of the M1-M4 dioxygenated metabolites with m/z values at 380. (B) Polymorphic CYP3A4.4 also produces a novel product (M5) compared to the wild type, and significantly less of the M6-M9 products with m/z values at 364.

Figure 5. Investigation of the novel M5 peak as an epoxide. Reactions were performed using the reconstituted system as described in Material and Methods. Reaction mixtures contained CYP3A4.4 (50 pmol) with (---) and without (—) epoxide hydrolase (25 pmol) and were incubated for 2 hours at 37^{o}C. Peaks were normalized to the AEA peak (not shown). The addition of epoxide hydroxylase did not cause a decrease in the signal for M5, but did result in the expected significant decreases in the peaks for M6, M7, and M8, which have previously been shown to be epoxides, with the concomitant formation of the four new diol products (M10-M13) with m/z values at 382 (Snider et al., 2007).

Figure 6. Incubation of the novel metabolites of CYP3A4.4 having peaks at m/z 380 with prostaglandin D synthase. Reactions were performed as described in Materials and Methods. Reaction mixtures were incubated with (---) or without (—) 5 μg of PGDS for 30 minutes at room temperature. Peaks were normalized to the AEA peak (not shown). The addition of PGDS causes a decrease in peaks M1-M4 and the formation of a new peak (M14)(m/z 381).

Figure 7. UV-visible spectra of CYP3A4.1 and CYP3A4.4 at 1 μM. Spectra were measured from 350 to 700 nm on a UV-visible spectrophotometer as described in Materials and Methods. CYP3A4.1 (❍) exhibited a mix between high and low spin forms and CYP3A4.4 was (△) more low spin.

Figure 8. Rates for the reduction of CYP3A4 wild type and mutant as determined by stopped-flow spectrophotometry. The reconstituted CYP3A4.1 (A) and CYP3A4.4 (B) and CPR solution (3 mM each) in the presence (filled) or absence (empty) of 100 μM testosterone were rapidly mixed with 0.1 mM NADPH solution in the stopped-flow spectrometer as described in Materials and Methods. The reduction of the P450s was monitored at 450 nm.

Figure 9. Metabolic products of AEA formed by CYP3A4.1 and CYP3A4.4.As shown here both CYP3A4.1 and CYP3A4.4 produce the four epoxide molecules 5,6-,8,9-,11,12-, and 14,15- EET-EA. In addition, CYP3A4.4 also catalyzes the formation of one monoxygenated product (believed to be 19-HETE-EA) as well as four dioxygenated products that are thought to be the peroxides shown here.

Table 1. Kinetic values for the metabolism of anandamide by CYP3A4.1 and CYP3A4.4.

Km and Vmax values were determined from the data in Figure 2 following 20-min incubations at 37^{o}C of 0.5-ml reaction mixtures containing reconstituted P450 CYP3A4.1 or CYP3A4 as described in Materials and Methods. Reaction mixtures contained 50 mM HEPES buffer, pH 7.4, AEA (1-256), and NADPH (1.2 mM) and the data represent the average of six experiments. Rates of formations were determined as described under Materials and Methods.

P450 3A4 Allele	Product Formed	V_{max} (sec^{-1})	K_m (μM)	V_{max}/K_m ($sec^{-1}/\mu M$)
*1	5.6 EET-EA	0.69	118	0.006
*4	5.6 EET-EA	0.23	108	0.002
*1	8.9 EET-EA	0.85	48	0.018
*4	8.9 EET-EA	0.53	98	0.005
*1	11.12 EET-EA	2.56	118	0.022
*4	11.12 EET-EA	0.90	76	0.012
*1	14.15 EET-EA	2.13	80	0.027
*4	14.15 EET-EA	1.10	85	0.013

Figure 1

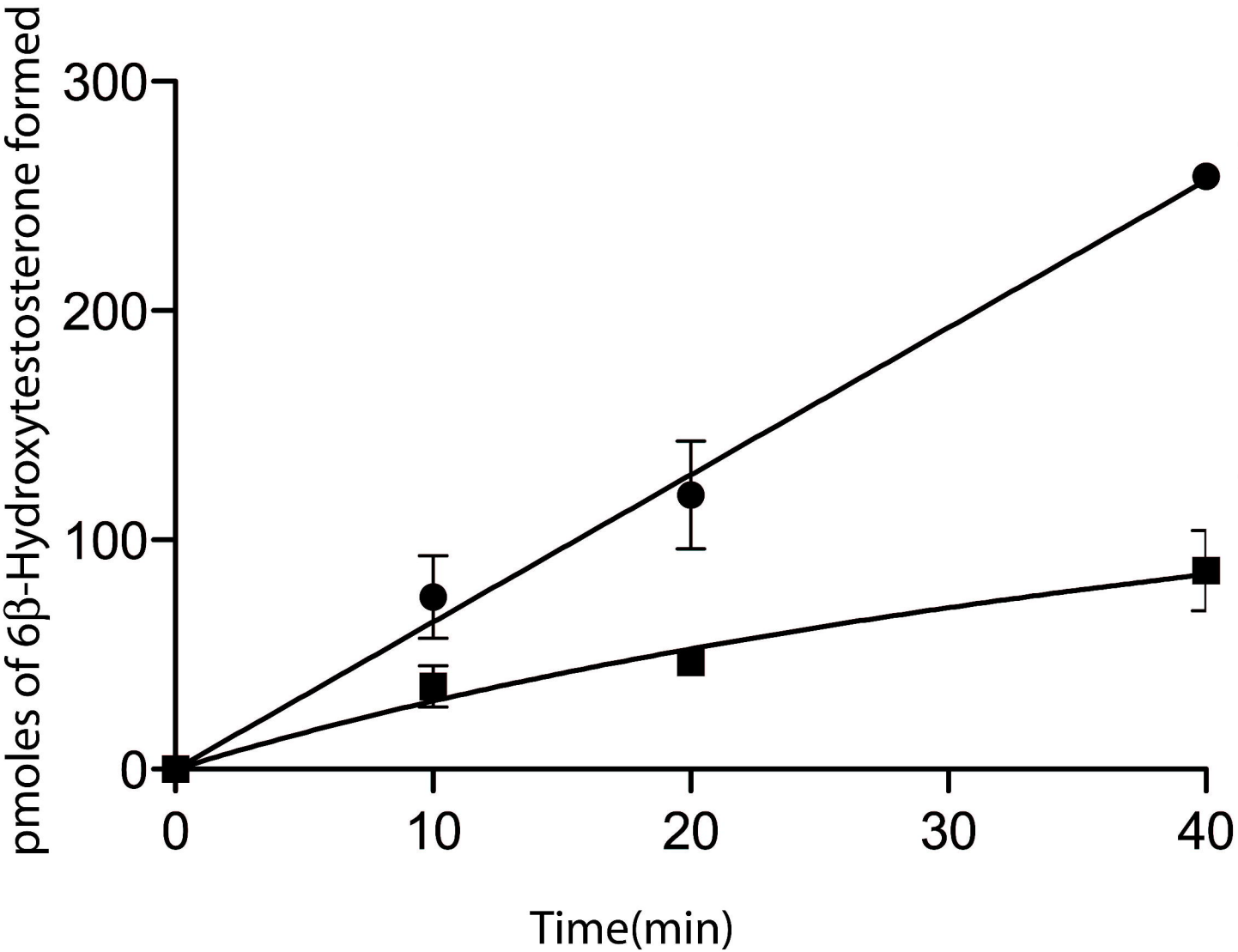

Figure 2

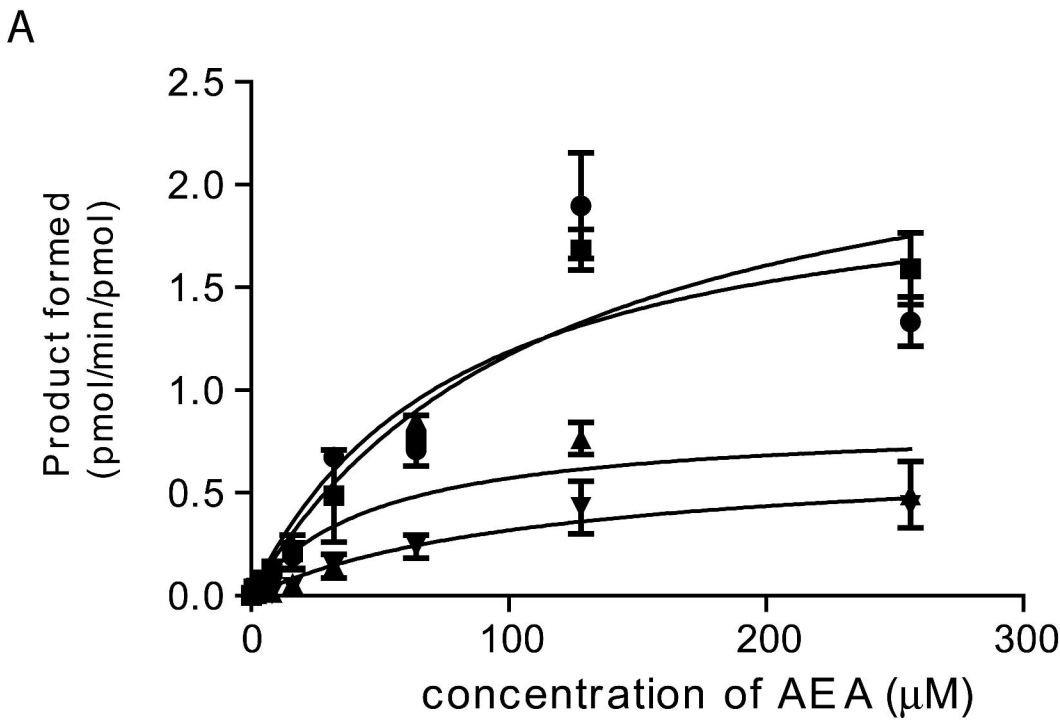
A
Product formed
(pmol/min/pmol)
2.5
2.0
1.5
1.0
0.5
0.0
0
100
200
300
concentration of AEA (μM)

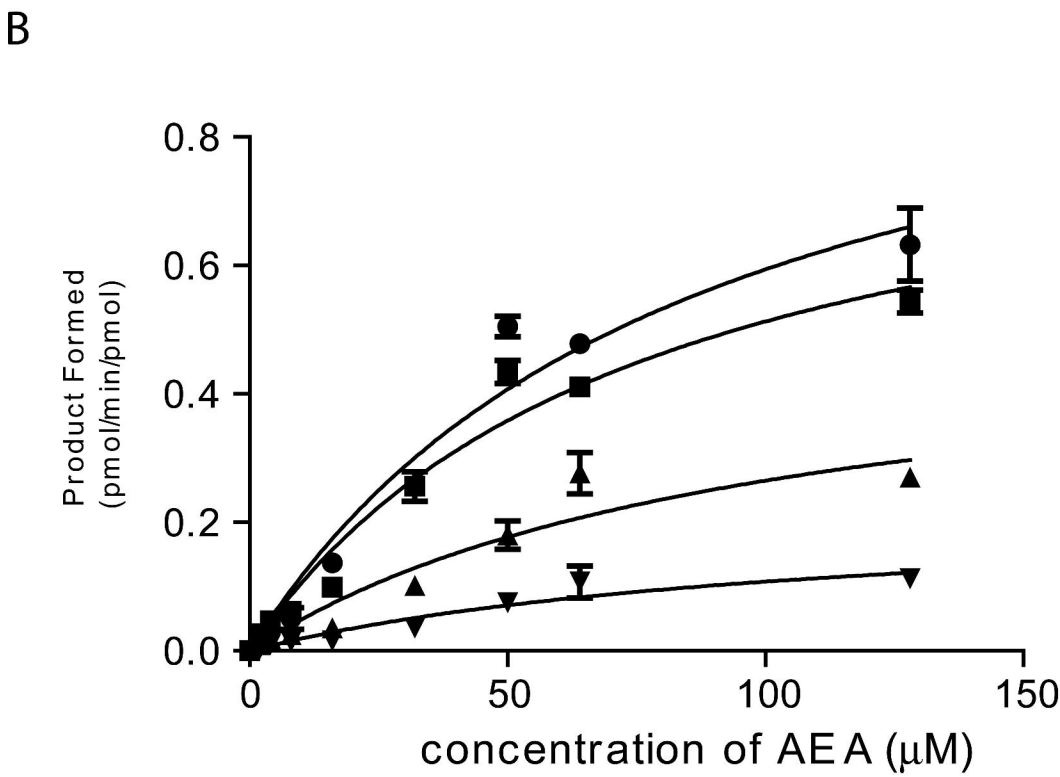
B
Product Formed
(pmol/min/pmol)
0.8
0.6
0.4
0.2
0.0
0
50
100
150
concentration of AEA (μM)

Figure 3

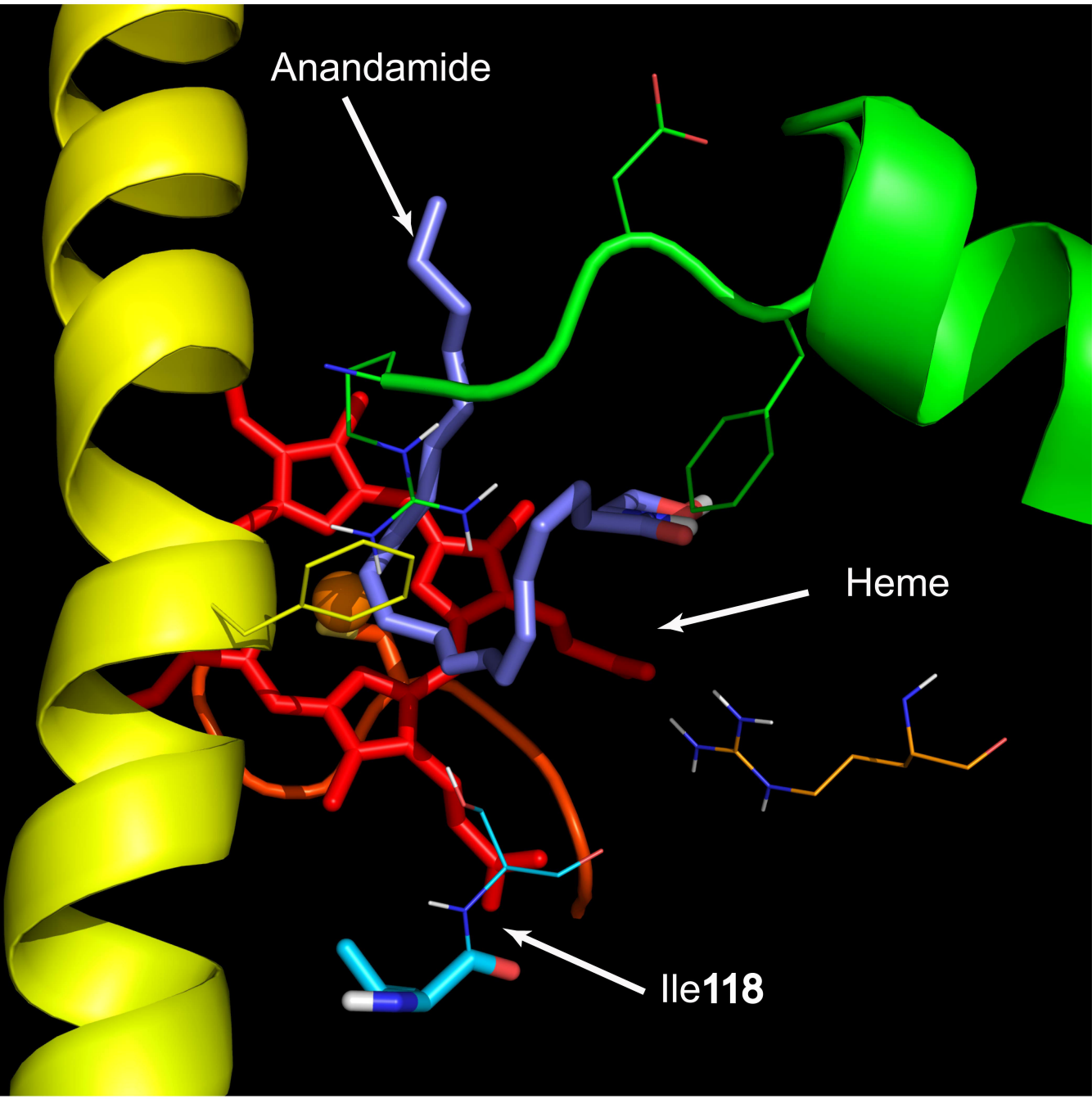

Figure 4

A

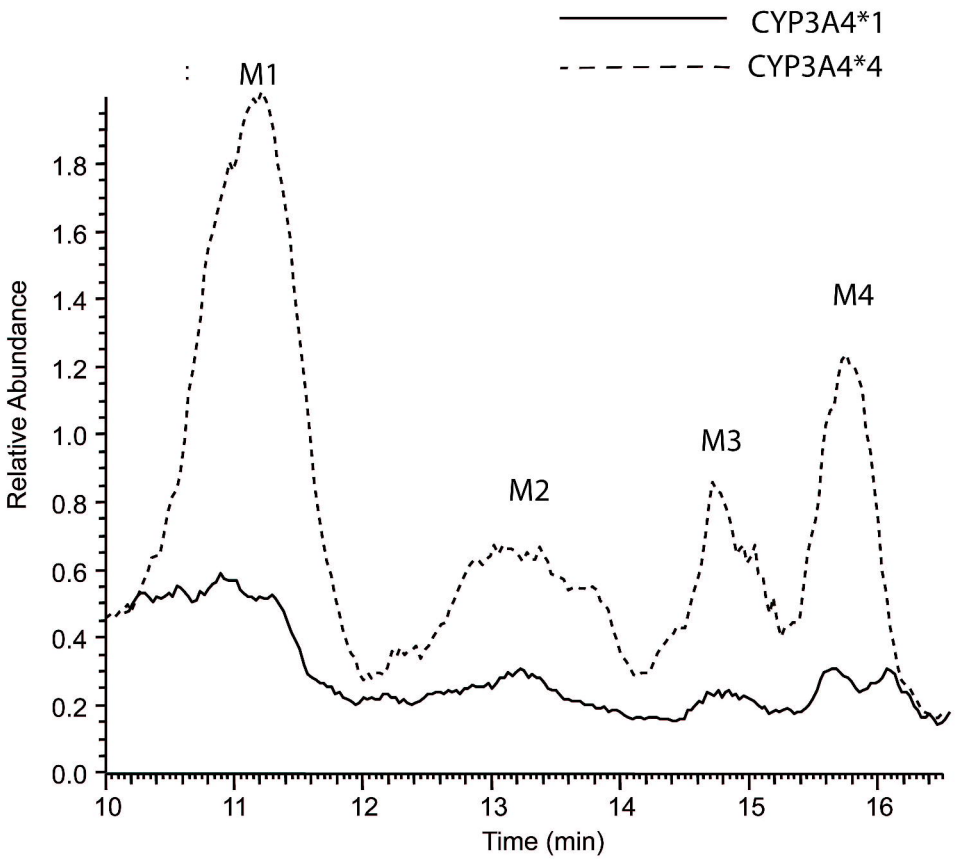
CYP3A4*1
CYP3A4*4
M1
M2
M3
M4
Relative Abundance
Time (min)

B

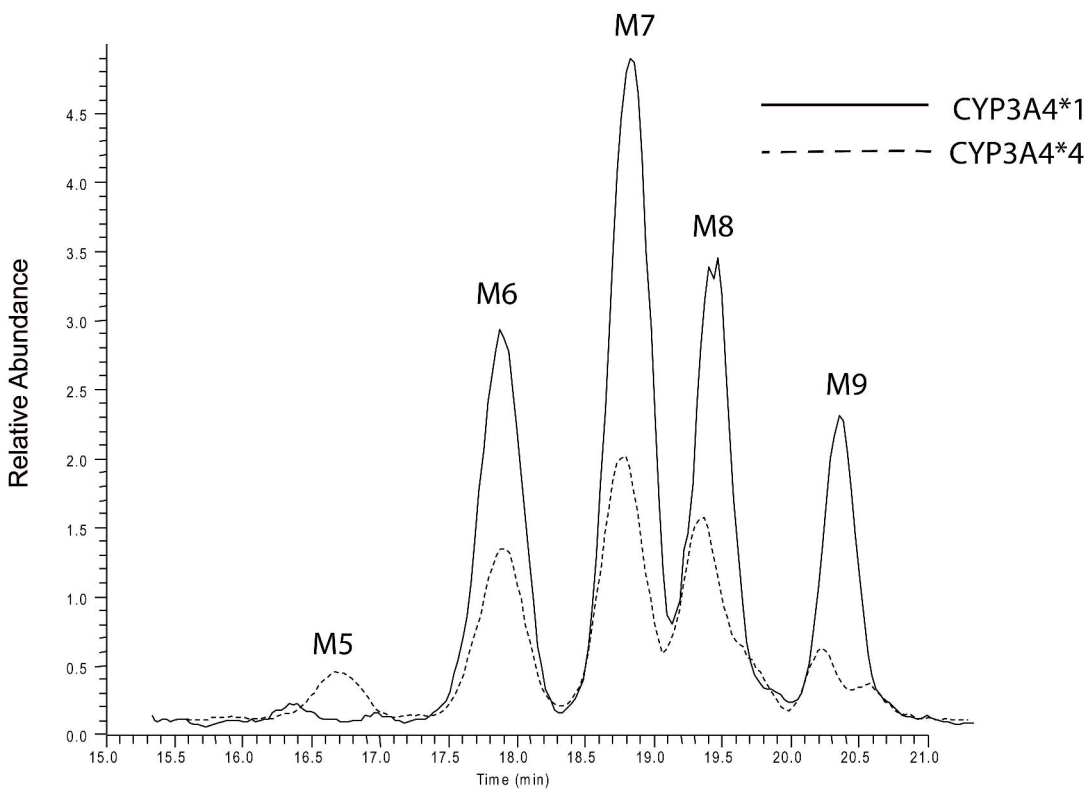
M5
M6
M7
M8
M9
CYP3A4*1
CYP3A4*4
Relative Abundance
Time (min)

Figure 5

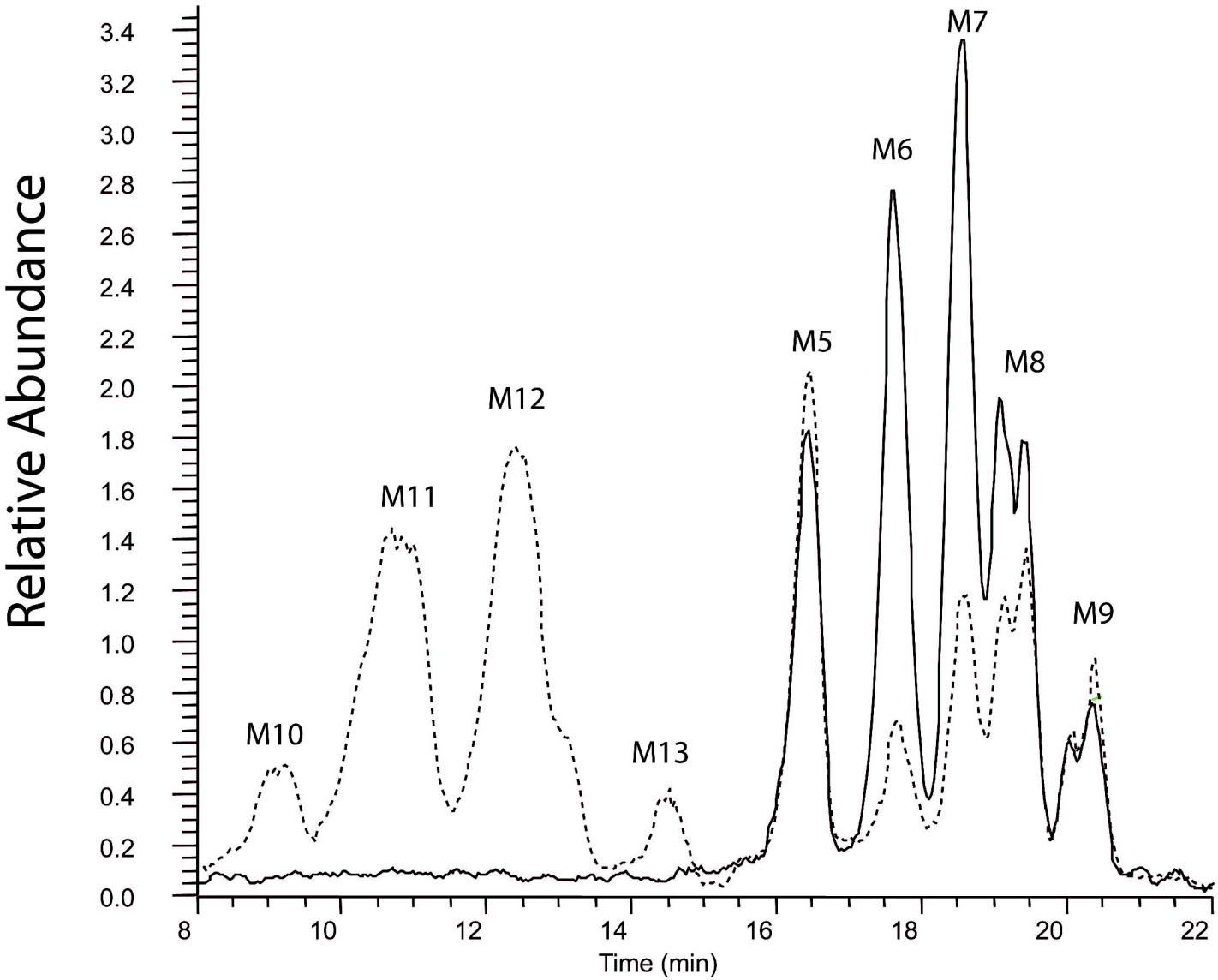

Figure 6

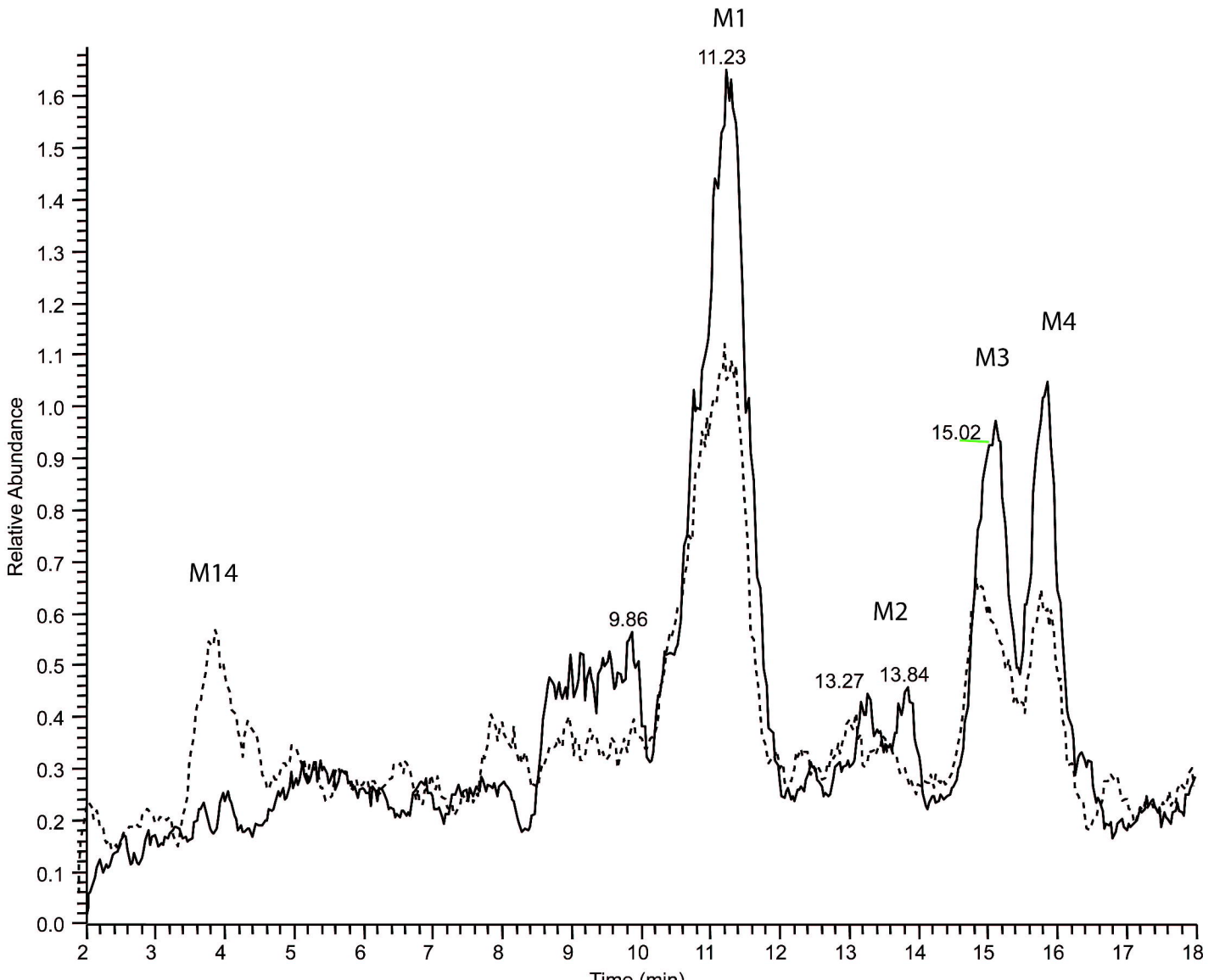

Figure 7

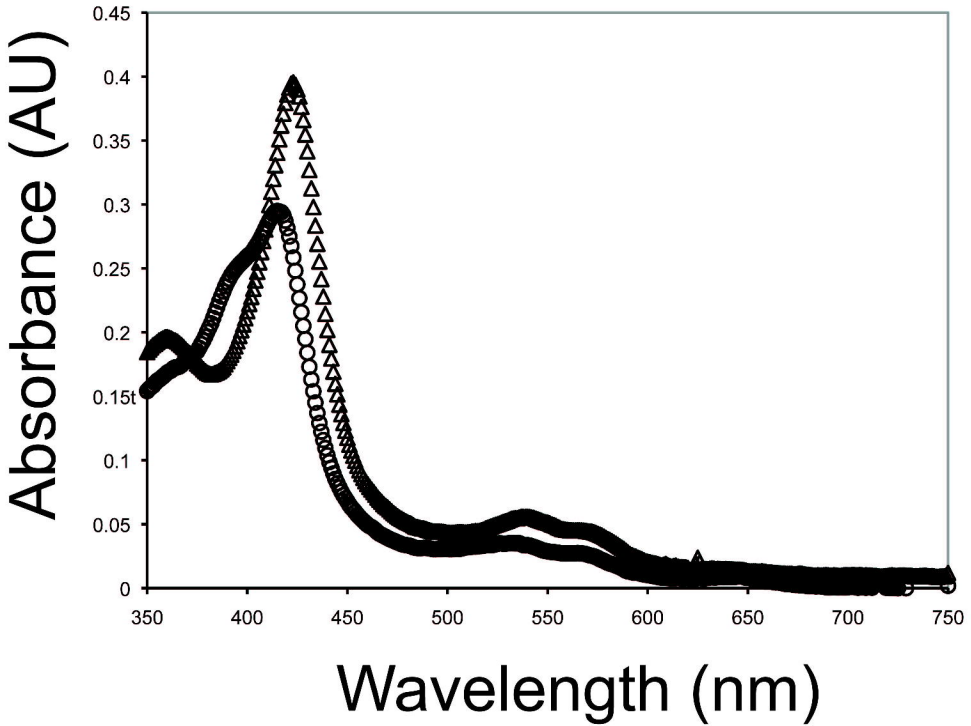
Absorbance (AU)
0.45
0.4
0.35
0.3
0.25
0.2
0.15t
0.1
0.05
0
350
400
450
500
550
600
650
700
750
Wavelength (nm)

Figure 8

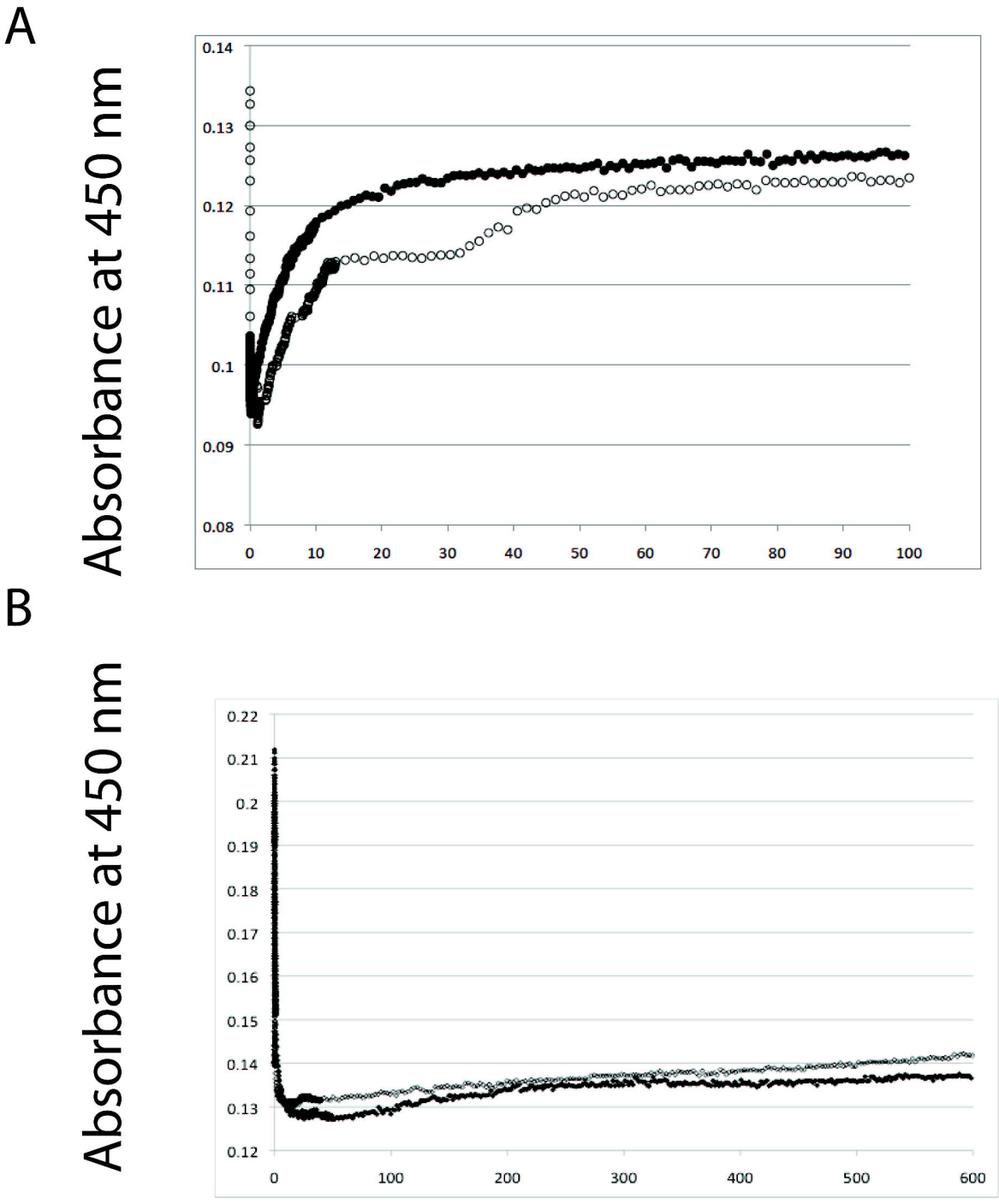

Figure 9

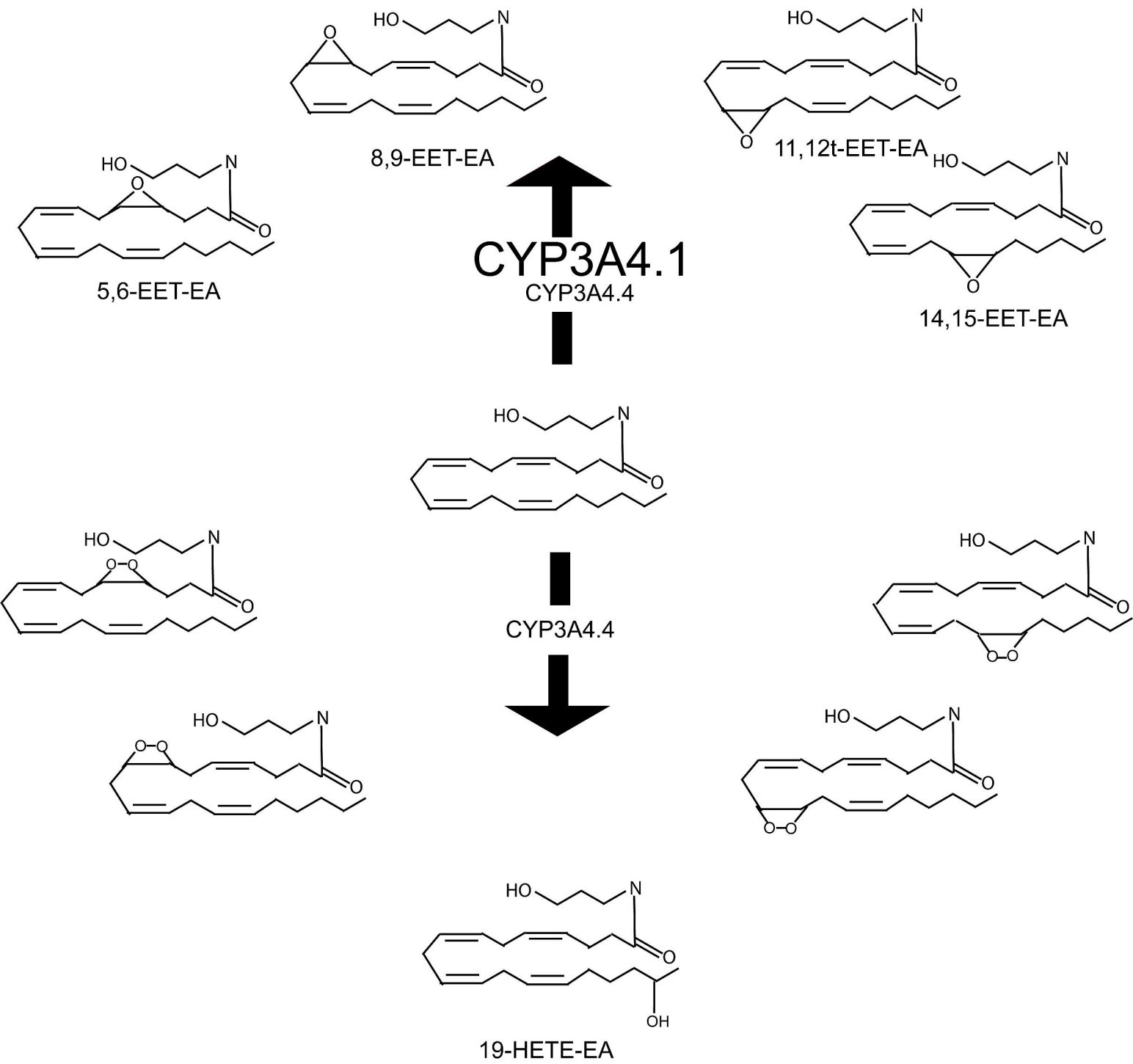
8,9-EET-EA
11,12t-EET-EA
5,6-EET-EA
CYP3A4.1
CYP3A4.4
14,15-EET-EA
CYP3A4.4
19-HETE-EA